

Formation and characterization of Y : 247 film through spray pyrolysis technique

SUMAN ANAND* and O N SRIVASTAVA

Department of Physics, Banaras Hindu University, Varanasi 221 005, India

*Present address: Optical Radiation Standards, National Physical Laboratory, New Delhi 110 012, India

MS received 8 May 2002; revised 17 February 2004

Abstract. The synthesis of high temperature superconducting films of Y : 247 ($T_c \sim 73$ K) have been successfully achieved. The difficulty in synthesis owing to narrow range of stability of Y : 247 has been taken care of through several quenching modes, e.g. quenching of the films synthesized at $\sim 850^\circ\text{C}$, in air or in liquid nitrogen. The energy dispersive analysis of X-rays (EDAX) and transmission electron microscopy (TEM) studies of the as processed film, $\text{Y}_2\text{Ba}_4\text{Cu}_7\text{O}_{14+x}$, exhibit nearly correct cationic stoichiometry of 2 : 4 : 7; also narrow regions ($< 50 \text{ \AA}$) of minority Y : 124 phase and stacking faults capable of working as flux pinning sites have been invariably found to be present. In addition to Y : 247, Ag admixed films have also been investigated. The T_c here is $\sim 70\text{--}75$ K which is similar to that of the film without silver. Representative estimates of transport critical current density (J_c) for Y : 247 films is $\sim 10^3 \text{ A/cm}^2$, and with silver corresponding to $\text{Y}_2\text{Ba}_4\text{Cu}_7\text{O}_{14+x}(\text{Ag}_{0.1})$ is found to be $\sim 10^4 \text{ A/cm}^2$.

Keywords. Thin film; quenching; superconducting.

1. Introduction

Three high-temperature superconductors are found to exist in the Y–Ba–Cu–O HTSC family. Their chemical formulae may be written as $\text{Y}_2\text{Ba}_4\text{Cu}_{6+n}\text{O}_{14+n}$, where n is the average number of CuO ‘chains’ separating two CuO_2 ‘planes’ in each basic building block. The $n = 0$ member of the family (‘Y : 123’) is the well known superconductor ($T_c \sim 90$ K). In contrast to Y : 123, the $n = 2$ member of the YBCO family (‘Y : 124’) is characterized by high stability of the oxygen concentration. In a co-existing manner, its critical temperature (T_c), 81–82 K, is quite stable (Karpinski *et al* 1990). The $n = 1$ member of this family i.e. $\text{Y}_2\text{Ba}_4\text{Cu}_7\text{O}_{14+x}$, was first synthesized under high oxygen pressure by Karpinski *et al* (1998). The Y : 123, Y : 124 and Y : 247 phases of Y–Ba–Cu–O along with their rare earth analogues offer three isostructural families with incremental variations in the lattice parameters, superconducting properties and potential advantages. Bordet *et al* (1998) determined the crystal structure of Y : 247, the structure contains alternating blocks with Cu–O single chains (Y : 123 units) and Cu–O double chains (Y : 124) units in the c direction.

Y : 247 can be prepared in a similar fashion as Y : 124, by employing oxygen enhancer catalysts or under high oxygen pressures, the primary differences between the

two preparation methods being the sintering temperature which in the case of Y : 247 is between 845°C and 870°C i.e. at intermediate temperature between those of Y : 123 and Y : 124. As is well known, $\text{Y}_1\text{Ba}_2\text{Cu}_3\text{O}_{7-d}$ has a variable oxygen stoichiometry, $0 \leq d \leq 1$, due to labile oxygen in the chain layer. In contrast, $\text{Y}_1\text{Ba}_2\text{Cu}_4\text{O}_8$ has a fixed oxygen stoichiometry ($d = 0$) due to the stable $-\text{Cu}_2\text{O}_2-$ ribbons. The Y : 247 phase has only about half the expansion anomaly of Y : 123 and suffers from nearly half the oxygen unloading shortcoming. Even more importantly, the material remains orthorhombic across the whole oxygen stoichiometric range and, therefore, is free from the rather subtle tetragonal to orthorhombic transition which is the cause of extensive microcracking in Y : 123. Another interesting aspect of Y : 247 phase seems to be the fact that unlike Y : 123 and Y : 124, the as grown phase of this HTSC material invariably contains some amount (few unit cell wide regions) of Y : 124. This second phase may be useful since it may act as flux pinning sites as it possesses the desired properties e.g. extent of few unit cells only. The Y : 124 phase has T_c close to 80 K, while that of Y : 247 depends on the oxygen stoichiometry and according to earlier reports has been observed at temperatures higher than 90 K (Tallon *et al* 1990). These features distinguish Y : 247 from its counterparts Y : 123 and Y : 124, and imparts special characteristics in regard to deployment for applications. As is well known now, thin films are better suited for a variety of applications. These applications include superconducting quantum interfer-

*Author for correspondence

ence devices (SQUIDS), superconducting interconnects and microwave application and in the measurement of their basic intrinsic properties. The most extensive studies on thin films employing both the conventional (e.g. chemical techniques like spray pyrolysis) as well as sophisticated techniques (e.g. laser ablation) have been carried out on Y:123 HTSC phase, some studies on thin films of Y:124 have also been done (Guptasarma *et al* 1991; Kumari Suman *et al* 1996). However, hardly any studies on thin films of Y:247 HTSC phase are available. In view of the lower variation of oxygen stoichiometry, absence of tetragonal to orthorhombic transition and the native presence of a minority (Y:124) phase, interest in the synthesis and studies of Y:247 films is imperative. Keeping these facts in view, the present investigations on the formation, synthesis and characterization of Y:247 films have been undertaken. The chemical technique of spray pyrolysis which is simple to handle, economically viable and yet leads to a device grade HTSC film and also holds technical potential (Deluca *et al* 1993), has been employed for the formation of Y:247 films.

Since the films corresponding to Y:247 HTSC phase have not been prepared earlier, the formation parameters are not known and Y:247 has a narrow stability range of existence as compared to other HTSC phases of the series, $Y_2Ba_4Cu_{6+n}O_{14+n}$ (e.g. Y:124, Y:123). The conditions of the formation of Y:247 thin films have been determined in the present investigation based on a series of quenching experiments in air and liquid nitrogen, aimed at arresting the Y:247 phase in the as synthesized films. In addition to quenching experiments, several annealing experiments in oxygen ambient were carried out for oxygen loading, and for the optimization of the transition temperature, T_c . The estimates of J_c for the Y:247 and Y:247 (Ag_{0.1}) films have also been obtained.

2. Experimental and results

Films of Y:247 were prepared by downward spray of a 0.3 M alcoholic solution containing the nitrates of Y, Ba and Cu in the atomic ratio 2:4:7, on single crystal MgO substrates. 5% of NaNO₃ was added as oxygen enhancer. The substrate temperature (T_s) for deposition was kept at

$450^\circ \pm 10^\circ\text{C}$. The oxygen was used as the carrier gas and the deposition rate was ~ 4 cc/min. As prepared films on the substrate were annealed at $850^\circ \pm 5^\circ\text{C}$ in O₂ atmosphere for different durations: ranging from 5–24 h. Keeping in view the fact that Y:247 will convert into Y:124 at temperatures below 850°C , in the first set of experiments the above annealed films were air quenched through quick withdrawal from the furnace. To have still better phase retention, in the second set of experiments the films were quenched in liquid nitrogen. The conversion of Y:247 into Y:124 is kinetically hindered below $\sim 650^\circ\text{C}$; therefore, the samples were oxygen loaded by slow heating in oxygen at $\sim 550^\circ\text{C}$ for 8 h, to achieve proper oxygen stoichiometry.

The quenching was performed in the following way: each ceramic sample was contained in a alumina boat and was heated to 850°C in flowing O₂. At quenching temperature ($T_q \approx 850^\circ\text{C}$), the samples with the boat was withdrawn rapidly (in < 1 s) and dropped directly into liquid nitrogen (LN), which was used because of its non-reactivity with the ceramic material. After quenching in LN, the film together with substrate was instantly heated to just above 100°C to get rid of any condensed moisture. Details of the main processing parameters embodying air or LN quenching and oxygen annealing (loading) are shown in tables 1 and 3. In an effort to get better results and also to compare the effect of air or LN quenching, another set of experiments were carried out in which the quenched films were annealed in Argon atmosphere (table 2).

The gross phase identification was carried out using Philips PW-1710 power diffractometer with a wide-angle goniometer and graphite monochromator. The XRD of the samples annealed at 850°C in oxygen, air quenched and then annealed in O₂ showed that in addition to Y:247, the other Y bearing phases i.e. Y:124 and Y:123, were also present. The comparative XRD patterns of the films annealed at 850°C in oxygen, quenched in air or LN and then subsequently annealed in Argon, are shown in figures 1a and b. It exhibits that the phase is nearly Y:247 with some traces of Y:124 and CuO. However, the XRD of the as grown samples annealed at 850°C in oxygen for 17 h, quenched in LN and then finally oxygen loaded at

Table 1. Details of processing parameters embodying air quenching.

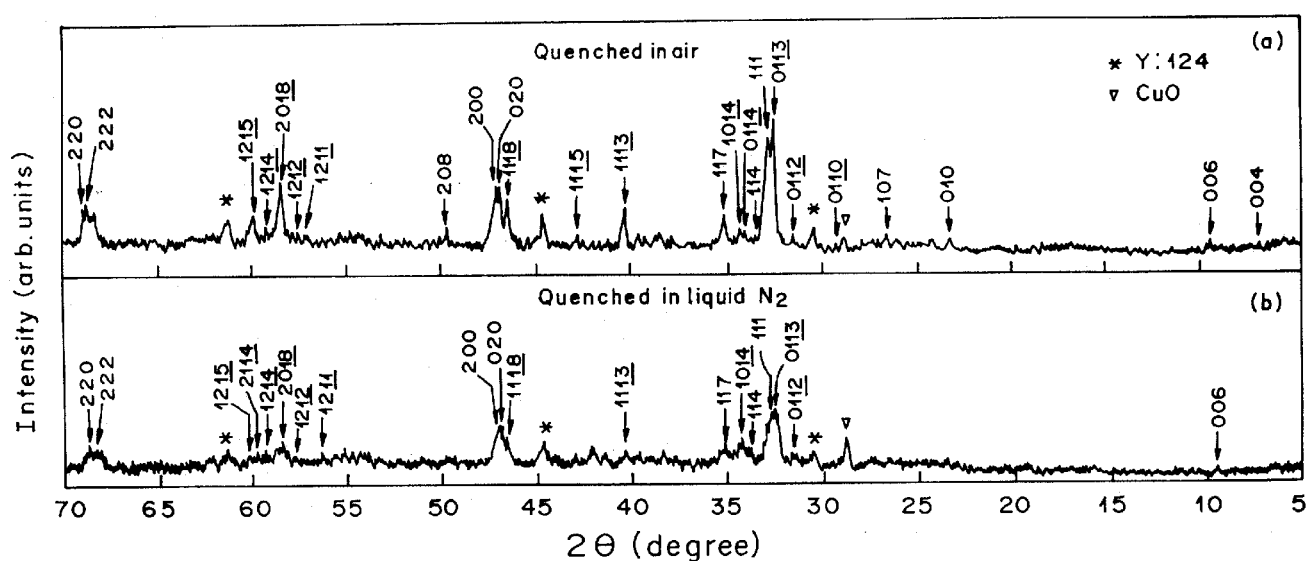
Annealing temp. ($\pm 5^\circ\text{C}$)	Annealing time in O ₂ (h)	Quenching medium	Temp. ($\pm 5^\circ\text{C}$)	Ambient	Annealing time	T_c ($R=0$) ($^\circ\text{K}$)
850	5	Air	500	Oxygen	12 h	–
850	10	Air	500	Oxygen	12 h	< 20 K
850	12	Air	550	Oxygen	8 h	< 47 K
850	14	Air	550	Oxygen	8 h	< 20 K
850	17	Air	550	Oxygen	8 h	< 20 K
850	24	Air	550	Oxygen	8 h	< 20 K

Table 2. Dependence of T_c on quenching medium.

Annealing temp. ($\pm 5^\circ\text{C}$)	Annealing time in O_2 (h)	Quenching medium	Temp. ($\pm 5^\circ\text{C}$)	Ambient	Annealing time	T_c ($R=0$) ($^\circ\text{K}$)
850	12	Air	550	Argon	8 h	~ 60 K
850	12	Liquid N_2	550	Argon	8 h	~ 40 K

Table 3. Dependence of T_c on annealing time embodying liquid N_2 quenching.

Annealing temp. ($\pm 5^\circ\text{C}$)	Annealing time in O_2 (h)	Quenching medium	Temp. ($\pm 5^\circ\text{C}$)	Ambient	Annealing time	T_c ($R=0$) ($^\circ\text{K}$)
850	14	Liquid N_2	550	Oxygen	8 h	~ 50 K
850	17	Liquid N_2	550	Oxygen	8 h	~ 73 K
850	24	Liquid N_2	550	Oxygen	8 h	~ 60 K

**Figure 1.** (a)–(b) XRD of Y:247 phase ($\sim 850^\circ\text{C}$; 12 h, after air quenching, annealed in Argon at $\sim 550^\circ\text{C}$ for 8 h) exhibiting some traces of Y:124 and CuO.

550°C , revealed better Y:247 phase formation evidenced through the presence of low angle reflections (e.g. 004, 006) of Y:247 as shown in figure 2.

Electrical characterization of the films was carried out using a Keithley resistivity set-up and an APD closed cycle refrigerator controlled by a computer. The R – T measurements for as grown films annealed at $\sim 850^\circ\text{C}$ for 12 h in O_2 , quenched in air or LN and then finally annealed in Argon showed T_c ($R=0$) ~ 60 K (curve a) and ~ 40 K (curve b), respectively (figure 3). The curve b i.e. LN quenched and Argon annealed sample, exhibited semiconducting behaviour before transition. The representative R – T curve obtained from the film annealed at $\sim 850^\circ\text{C}$ for ~ 17 h in O_2 , LN quenched and then finally oxygen loaded, exhibited pre-transition metallic behaviour and showed T_c ($R=0$) of ~ 73 K (figure 4). Following the same method applied for the synthesis of Y:247

films, the silver bearing Y:247 films were also prepared. However, for introducing Ag, suitable amount of 0.3 M AgNO_3 solution in distilled water was added in the main solution. For the case of Ag bearing Y:247 phase, a representative R – T curve is shown in figure 5, the T_c ($R=0$) corresponding to this curve comes out to be ~ 75 K.

For HTSC materials, which correspond to rather complex ceramic materials, in addition to the gross structure, monitoring of the local area structure and microstructures, are equally important. Keeping in view the fact that the transmission electron microscopy (TEM) is the most appropriate technique for the said purpose, we employed TEM technique both in imaging and diffraction modes (and also EDAX) for the exploration of local area structure/microstructure. A computerized electron microscope (Philips EM (CM-12)) was used both in imaging and diffraction modes for microstructural analysis. Samples for

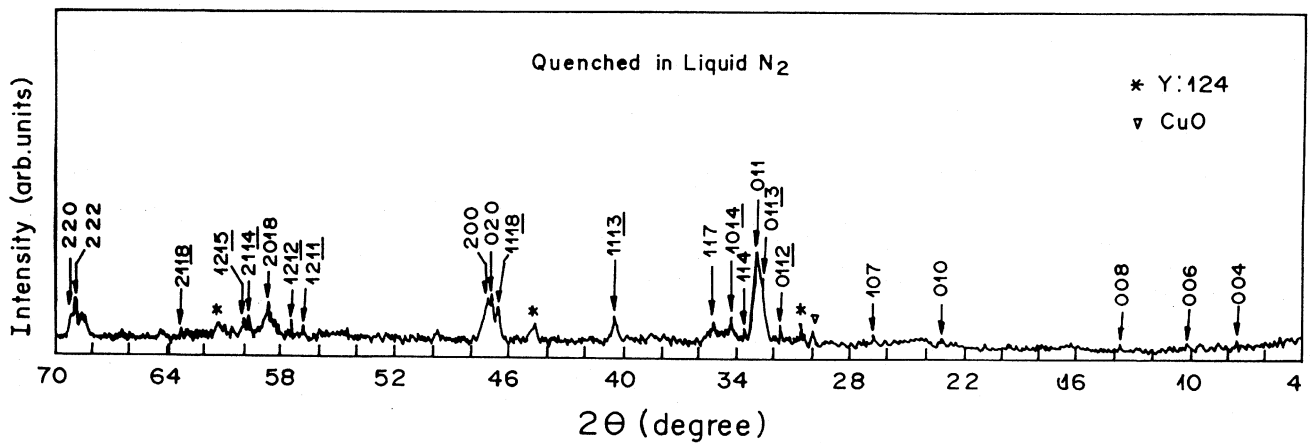


Figure 2. XRD pattern of the spray pyrolysed Y:247 phase ($\sim 850^\circ\text{C}$; 17 h, oxygen loaded at $\sim 550^\circ\text{C}$).

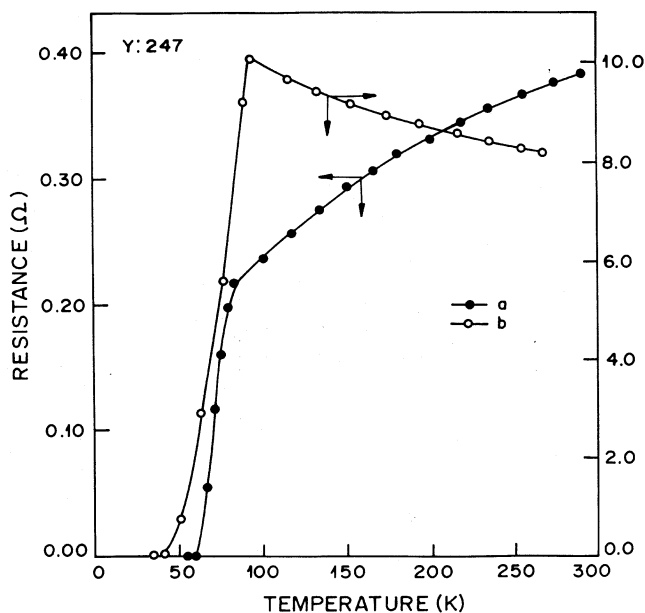


Figure 3. Temperature dependence of the resistance of (a) air quenched and (b) LN quenched, samples annealed in Argon.

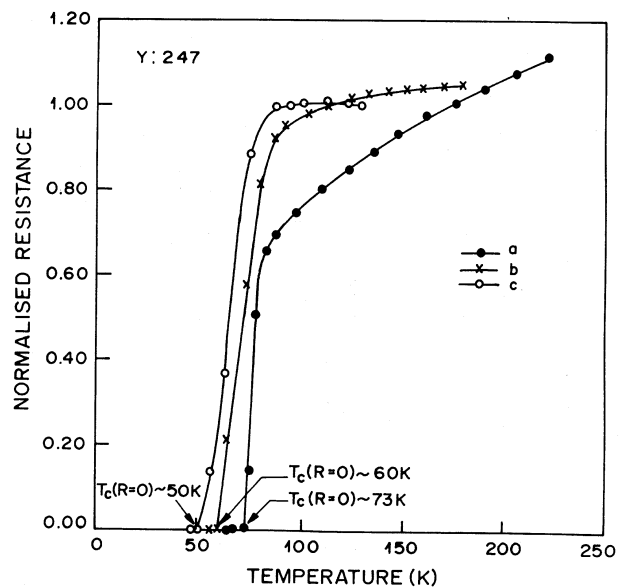


Figure 4. Variation of resistance with temperature for the films quenched in LN after annealing at 850°C in oxygen for (a) 17 h, (b) 24 h and (c) 14 h.

TEM studies were made by scraping the as synthesized Y:247 over carbon coated copper grids. Figure 6 shows EDAX of the processed Y:247 film. The composition ratio of Y:Ba:Cu as determined is approximately 2:3.5:7.3. The EDAX results indicate good agreement with the envisaged 2:4:7 stoichiometry. A typical electron diffraction pattern and TEM image bringing out direct lattice resolution representative of the as processed sample are shown in figures 7 and 8, respectively. Figure 7a exhibits the SAD pattern, in which besides the sharp diffraction spots, a weak diffuse streaking along c^* can also be seen. Yet another curious structural feature as revealed by the electron diffraction studies is the presence of a superstructural phase with $c' \cong 4c_0$ (c_0 being the lattice param-

eter of the parent Y:247 phase). However, irrespective of streaking the presence of some closely spaced spots along the marked direction reflects the fact that unit cells of c periodicity $\sim 50.8 \text{ \AA}$ ($c/2 \approx 25.4 \text{ \AA}$) which corresponds to Y:247 phase, are present (figure 7b). Figure 8 shows that the minority phase i.e. Y:124 (B), is embedded in the Y:247 regions (A).

3. Discussion

As mentioned earlier, the Y:247 structure consists of alternating Y:123 and Y:124 blocks. Due to the double Cu-O chains the coordination of oxygen in Cu increases

in the Y : 124, therefore, the oxygen is more stable than in the Y : 123 structures. In Y : 247 the oxygen in the single chains i.e. in the Y : 123 layers, is expected to be weakly bound, while the oxygen in the Y : 124 layers is more tightly bound. Consequently, the oxygen loss on heating Y : 247 should be less than for Y : 123 at the same temperature and oxygen partial pressure. In contrast to the Y : 123 phase, the Y : 247 HTSC phase remains superconducting (although with reduced T_c) even after losing an appreciable amount of oxygen from the Y : 123 like blocks. At higher temperatures, the Y : 124 blocks are destroyed too, leaving the Y : 123 and CuO as the only 'stable' products.

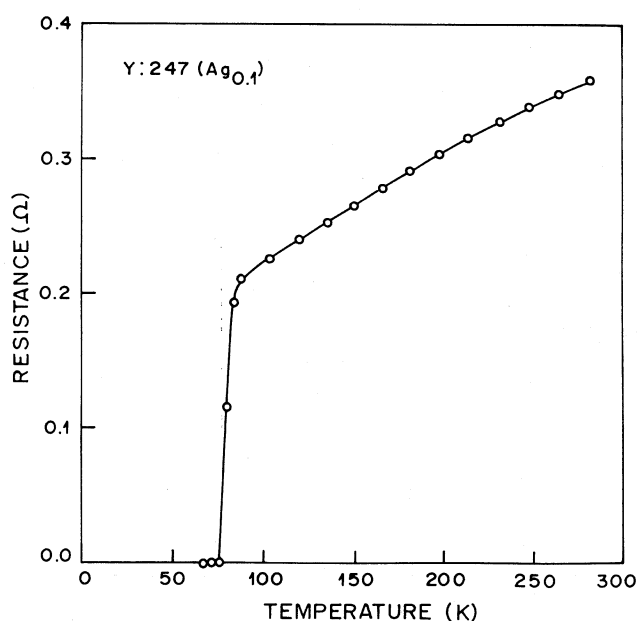


Figure 5. Variation of resistance with temperature for the Ag bearing Y : 247 films corresponding to $Y_2Ba_4Cu_7O_{14+x}$ ($Ag_{0.1}$).

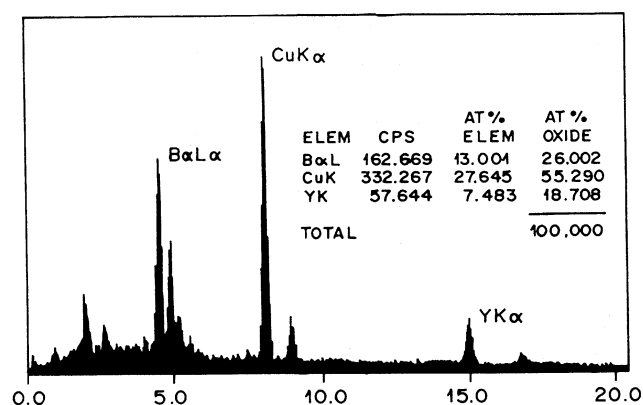


Figure 6. EDAX of Y : 247 thin film exhibiting the nearly correct cationic stoichiometry.

The thermal stability of each of these three phases (Y : 123, Y : 247 and Y : 124) is different. During annealing of the Y : 124 phase, a sudden decomposition with the formation of the Y : 123 phase starts at about 880°C. The Y : 124 phase has very high thermal stability and the Y : 247 phase is less stable than Y : 124 (but more stable than Y : 123) because of the existence of Y : 123 like blocks in the structure. These considerations reveal that Y : 247 is an intermediate phase between Y : 123 and Y : 124 and also the formation of Y : 124 and Y : 247 phases occurs via intermediate multiphase reactions with strong consumption of oxygen. In the present investigation the samples annealed at ~850°C for different time spans of 14, 17 and 24 h, have been quenched in liquid N_2 so as to arrest the formed phases. Since the thermal mass of the sample i.e. substrate and film, is small, the temperature would drop from ~850°C to nearly room temperature in a few seconds. It would thus be possible to freeze the phase prevalent at the processing temperature of ~850°C. The transition temperature, T_c , of the Y : 247 phase appears to vary in a wide range of 16–70 K (see tables 1–3). This variation presumably arises due to varying oxygen content. On the other hand, T_c of Y : 124 shows a very small deviation from 81 K (Kumari Suman *et al* 1996).

The critical current densities of the as-synthesized Y : 247 films were measured on several samples. The representative estimate of J_c was found to be ~2 to 3×10^3 A/cm². The critical current density, J_c , for the $Y_2Ba_4Cu_7O_{14+x}$ ($Ag_{0.1}$) films was found to be ~ 2×10^4 A/cm² i.e. about an order higher than the films without Ag. This is however, expected since in other Y bearing cuprate HTSC thin film phases e.g. $YBa_2Cu_3O_{14+x}$ (Ag_y) (Kumar *et al* 1993), J_c have been found to improve significantly with Ag doping. Further work on optimization of J_c including the effect of variation of Ag concentration is presently being carried out and results will be forthcoming.

In the present investigation attempts have been made to monitor the microstructural features by electron microscopy. From the microstructural investigations, it has been found that the as synthesized samples are generally biphasic. As a result of decomposition, Y : 247 may be partially converted into Y : 124. If the removal of a Cu–O chain is random, there would be a stacking disorder along 'c'. This disorder causes streaking in the diffraction pattern of the 00l rows of spots. The Y : 124 phase, if only few unit cells wide would have a much lower T_c than the usual bulk Y : 124. Thus narrow Y : 124 regions which would be compatible with the coherence length (~30 Å) are expected to act as flux pinning sites. Similarly stacking faults in the Y : 247 matrix (see figure 8) having widths of the order of coherence length would also act as flux pinning centres. The representative TEM image shown in figure 8 brings out the fact that narrow regions having extents of about the coherence length are present corresponding to both the Y : 124 and stacking faults.

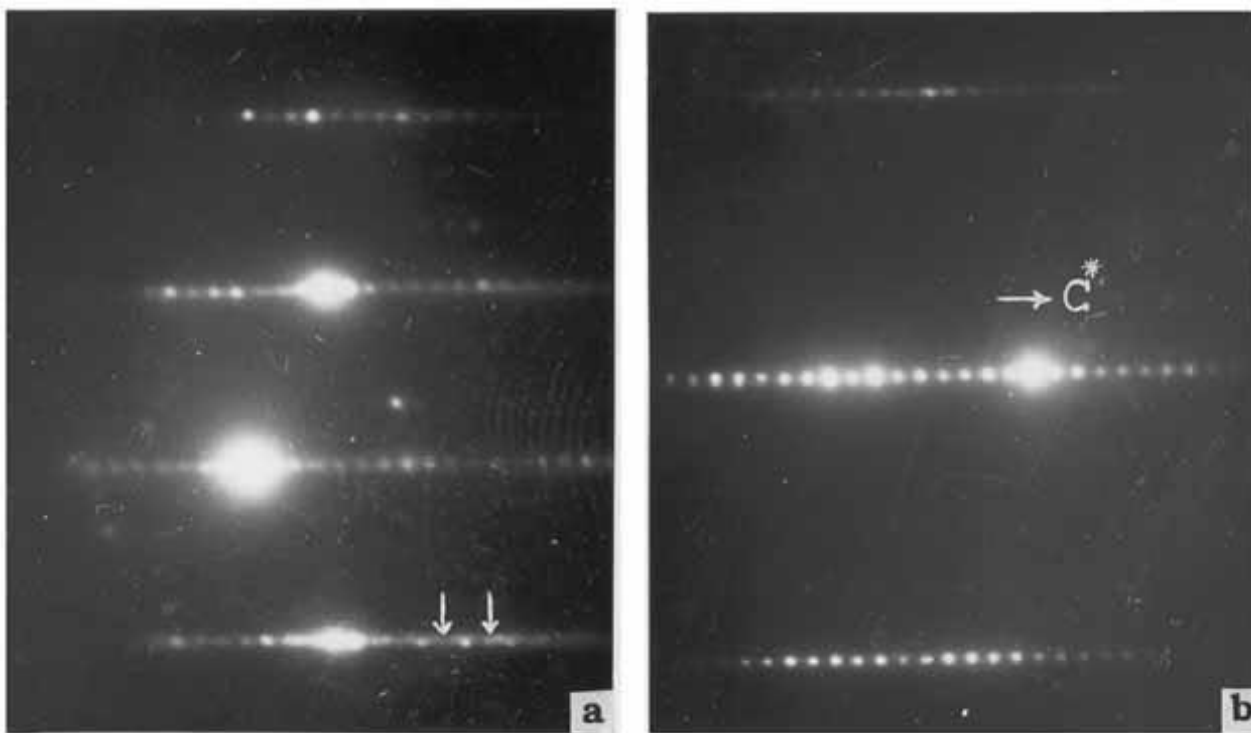


Figure 7. (a) SAD pattern exhibiting disorder through diffuse streaking along the c^* axis and superstructures ($c' \approx 4C_0$) marked by arrow and (b) a representative SAD pattern of Y:247 showing $c/2 \approx 25.4 \text{ \AA}$.

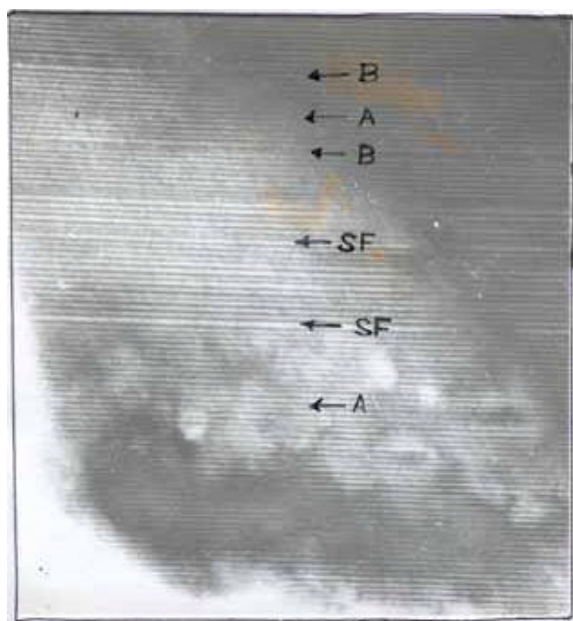


Figure 8. Lattice resolution TEM micrograph obtained from Y:247 film. Notice the presence of some minority phase, Y:124 (marked B) as also the stacking faults (marked SF).

Thus the as synthesized and processed Y:247 films appear to embody native flux pinning centre which enhance the intragrain critical current density.

4. Conclusions

It can thus be concluded that in the present study, Y:247 high temperature superconducting films with $T_c \sim 73 \text{ K}$ and $J_c \sim 10^3 \text{ A/cm}^2$ (for $\text{Y}_2\text{Ba}_4\text{Cu}_7\text{O}_{14+x}$ ($\text{Ag}_{0.1}$), the $J_c \sim 10^4 \text{ A/cm}^2$) have been successfully prepared through spray pyrolysis technique. The Y:247 phase has been retained through suitable quenching treatments in air or LN, from the temperature $\sim 850^\circ\text{C}$ representing the phase stability region of Y:247. From the local area structural and microstructural studies through TEM, it has been found that the as synthesized and processed films embody the minority Y:124 phase and stacking fault (SF) regions which have narrow widths compatible with coherence length, λ ($\sim 30 \text{ \AA}$) and thus the as prepared films are expected to contain effective flux pinning sites.

Acknowledgements

The authors are grateful to Dr Vikram Kumar, Director, National Physical Laboratory, New Delhi, Prof. A R Verma and Prof. R P Rastogi for encouragement. They also thank Dr A V Narlikar, Dr T V Ramakrishnan, Professor G V Subba Rao and Professor S B Ogale for discussions. The authors acknowledge financial support from DST (PMB-NSTB) and UGC.

References

- Bordet P, Chaillout C, Chenarans J, Hodean J L, Marezio M, Karpinski J and Kaldis E 1998 *Nature* **334** 596
- Deluca John A, Koras Pamela L, Tkaczyk J E, Bednarczyk Peter J, Garbaskas Mary F, Briant Clyde L and Sorensen Donald B 1993 *Physica* **C205** 21
- Guptasarma P, Palkar V R, Multani M S, Vijayaraghavan R, Bendre Subhash T and Ogale S B 1991 *Solid State Commun.* **79** 851
- Karpinski J, Rusiecki S, Kaldis E, Bucher B and Jilek E 1990 *Physica* **C160** 449
- Karpinski J, Beeli C, Kaldis E, Wisard A and Jilek E 1998 *Physica* **C830** 153
- Kumari Suman, Singh A K and Srivastava O N 1996 *Superconduct. Sci. and Technol.* **9** 405
- Kumar D, Sharon M, Pinto R, Apte P R, Rai S P, Purandare S C, Gupta L C and Vijayaraghvan R 1993 *Appl. Phys.* **62** 3522
- Tallon J L, Pooke D M, Buckley R G and Presland M R 1990 *Phys. Rev.* **B41** 7220